

# CRITICAL PLANES ANALYSIS OF THE IMPACT OF POROSITIES ON THE FATIGUE OF METAL SOLIDS

**Fauvin Françoise<sup>1</sup>, Ghadhab Roua<sup>1</sup>, Debono Gregory<sup>1</sup>, Bermond Antonin<sup>2</sup>, Carton Jean-François<sup>2</sup> and Feulvarch Eric<sup>1</sup>**

<sup>1</sup> Laboratoire de tribologie et dynamique des systèmes (LTDS)  
Ecole Centrale de Lyon, 69130 Ecully  
francoise.fauvin@enise.fr  
roua.ghadhab@enise.fr  
gregory.debono@enise.fr  
eric.feulvarch@enise.fr

<sup>2</sup> Safe Metal  
1 bd de la boissonnette, 42110 Feurs  
antonin.bermond@safe-metal.com  
jeanfrancois.carton@safe-metal.com

**Key words:** Fatigue, critical planes, porosities, cast steel.

**Abstract.** In this work, we take interest in the impact of defects present in metal solids manufactured by material fusion or by additive manufacturing on their fatigue life during cyclic loading. Indeed, we observe a more or less strong local plasticity around the defects even if the stresses remain below the elastic limit, which can strongly impact the fatigue life of such solids. In the case of a part obtained by steel casting, it is the retassures that make the part most vulnerable. In the case of solids obtained by additive manufacturing, the most damaging defects are surface roughness and porosities linked to a lack of fusion. In order to estimate the fatigue life of such solids, it is necessary to observe the states of stress and strain around the defects during a cycle. As stress levels can be relatively high locally, critical plane type criteria are relevant for estimating the fatigue life of such solids. In order to carry out a fatigue analysis of a part obtained by steel casting or by additive manufacturing, we propose to model it by finite elements, with a refinement of the elements around the porosities, then to calculate the local stress and strain states, and finally to implement a critical plane type criterion, like the Fatemi-Socie criterion. The critical planes are the planes on which the maximal shear strain amplitudes occur. The local stress and strain states can be highly multi-axial. So the determination of the critical planes can be very computationally and storage consuming. In the present work, an analysis in the space of deviators of the deformation tensor makes possible determination of such planes in each of the numerous nodes of the mesh. These three steps of calculation, correlated with experimental tests, makes it possible to envisage obtaining fatigue life laws for numerous metallic materials presenting defects.

## 1 INTRODUCTION

Nowadays, steel is the most used material in the world and its consumption practically reaches a billion tons per year. Traditionally, we distinguish between wrought steel and cast steel. Cast steel, which represents approximately 10% of total production, is a relatively recent material whose industrialization generally corresponds to the industrial revolution of the 19th century. In cast steel foundry, parts are obtained directly by solidification of the liquid metal in impressions (or molds) in refractory or metallic material, which reproduce as faithfully as possible the final shapes and dimensions of the parts requested by the users. This practice of “near net shape” is technically and economically interesting, because it eliminates costly subsequent machining operations and it makes it possible to preserve the raw foundry skin, which generally has a fine microstructure favorable to the good performance of the parts in service. This technique allows in particular production on an industrial scale of massive parts without shaping operations (such as parts of agricultural or construction machinery, parts used in the railway industry...). Another advantage of cast steels is that they allow the use of recycled material.

Parts manufactured in this way are subject to cyclical loading during their service. Fatigue phenomena must therefore be taken into account to certify their lifespan. The structure of foundry parts presents defects of three types: non-metallic inclusions, gaseous porosities and sinkholes, which can be eliminated on a macroscopic scale by modification of the design or finishing operations (heat treatment, welding...). Therefore these defects will remain present on the microscopic scale and we will refer to them as porosities. The presence of porosities will alter the fatigue resistance of mechanical parts as shown by the Murakami criterion or the Kitagawa-Takahashi diagram. In the Murakami criterion, the porosity is characterized by a length called area equal to the square root of the projected area of the porosity in the principal direction of the loading. This quantity makes it possible to determine a critical porosity size below which the endurance limit of the material is not compromised. The Kitagawa-Takahashi diagram illustrates how the length of the crack affects the endurance limit of materials, and it effectively complements the Murakami criterion by providing a visual framework for understanding the impacts of imperfections on fatigue resistance. This diagram brings together the three domains of microstructurally short, physically short and long cracks—and indicates for a given material how its endurance limit decreases as a function of crack length. It also shows the critical size of the crack from which this reduction becomes significant.

In his thesis work, in collaboration with the company Safe Metal, world leader in the manufacture of massive cast steel parts, Antonin Bermond studied the influence of the microstructure of steel G20Mn5 on the fatigue life of molded parts [1]. He was interested in “equivalent ellipsoid” type criteria to find a correlation between the shape of the porosity and its propensity to become a place of cracking. To verify their relevance for G20Mn5 cast steel parts, he carried out a test campaign on specimens subjected to cyclic loading with imposed plastic strain. He used tomography analysis of the specimens in order to study the dangerousness of the porosities in a non-destructive manner. He showed experimentally that the most harmful porosities

are sinkhole type porosities. Very dendritic in shape, these sinks can be compared to flattened plates or discs where their two main dimensions are very large compared to their thickness, thus confirming the work of Murakami and Kitagawa-Takahashi.

This work is a continuation of the thesis work of Antonin Bermond [2]. The objective is to propose a numerical analysis of the fatigue resistance of molded parts and G20Mn5 steel using a critical plane-type fatigue criterion, in order to take into account the strong multi-axiality around the porosities, as well as the strong local plasticity. This work proposes to start from the fine geometry of the porosities obtained by tomography, to calculate the stress and strain states around each porosity using the finite element method. The determination of the critical planes at each point of the mesh is then obtained by a rapid and efficient method developed by Fauvin & al [3]. This work is innovative because it makes it possible to obtain, in an industrially very interesting period of time, a map of the fatigue parameter involved in critical plan type criteria. It thus makes it possible to consider the development of a law between the lifespan of G20Mn5 cast steel parts and the value of the fatigue parameter. In this work, the choice fell on the Fatemi-Socie criterion, recognized as relevant in low and high-cycle fatigue [4].

## 2 Fatigue criterion

Uniaxial cyclic tests carried out on a series of specimens constitute the first step to characterize different fatigue behaviors of metallic materials. In our case, although each specimen is subjected to uni-axial loading along its axis, we note a strong multi-axiality near the porosities present in its microstructure. It is therefore important to use a multiaxial fatigue criterion in our study. Critical plane type criteria are widely used in the case where the principal directions of the stress and strain tensors vary during a loading cycle [5]. The critical planes are the planes of maximum damage along which the stress or strain shear amplitudes are maximum. In the sense of such criteria, the critical planes are the planes along which cracks begin. The critical plane type criteria propose to calculate at each point of the material, a fatigue parameter combining the amplitude of shear in stresses or strains with a magnitude normal to the critical plane. This parameter is then linked to a lifespan following a Manson Coffin type power law in low cycle fatigue or a Basquin type power law in fatigue with a large number of cycles.

If we consider a point of interest  $M$  of the material or mesh and a plane  $\mathcal{P}_n$  of normal  $\vec{n}$  around  $M$ , the history of the shear loading is described by a cloud of points in the plane  $\mathcal{P}_n$  in figure 1.

The shear amplitude  $\Delta\gamma_n$  in this plane is determined by the maximisation

$$\max_{(t_i, t_j)} \|\vec{\gamma}_n(t_i) - \vec{\gamma}_n(t_j)\| \quad (1)$$

Finding critical planes therefore amounts to solving the double maximization problem

$$\operatorname{argmax}_{\vec{n}} \max_{(t_i, t_j)} \|\vec{\gamma}_n(t_i) - \vec{\gamma}_n(t_j)\|$$

Determining critical planes can be very costly in terms of calculation time if we plan to scan all the planes around the point of interest. It was demonstrated by Fauvin & al [3] that, at each

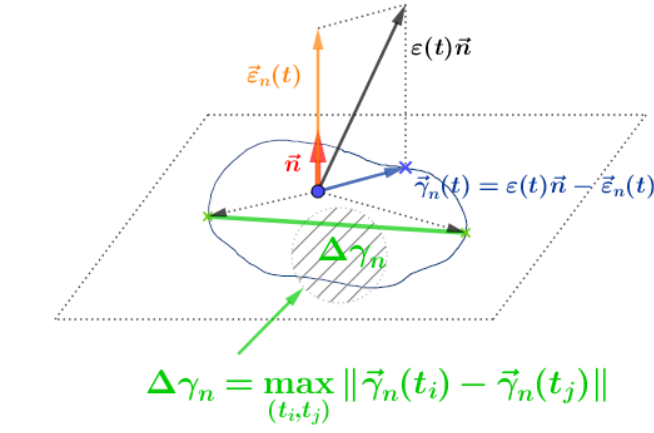


**Figure 1:** Shear amplitude in the plane of normal  $\vec{n}$

point of the material, the shear amplitude following a plane can be deduced from the history of loading in the space of the deviators of the stress or strain field, equipped with Tresca standard

$$\|\epsilon_D\|_{Tresca} = \max_{i \neq j} |\lambda_i - \lambda_j|$$

where  $\epsilon_D$  is a deviator tensor and  $\lambda_k$  its eigenvalues. The main idea of the demonstration lies in the permutation of the double maximization

$$\max_{\vec{n}} \max_{(t_i, t_j)} \|\vec{\gamma}_n(t_i) - \vec{\gamma}_n(t_j)\| = \max_{(t_i, t_j)} \max_{\vec{n}} \|\vec{\gamma}_n(t_i) - \vec{\gamma}_n(t_j)\| \quad (2)$$

if we note  $\epsilon_D(t_i)$  the deviatoric part of the strain tensor at time  $t_i$  of the stabilized cycle, the maximum value of  $\|\vec{\gamma}_n(t_i) - \vec{\gamma}_n(t_j)\|$  on the set of normal planes is given by the radius of the largest Mohr circle of the deviator  $\epsilon_D(t_i) - \epsilon_D(t_j)$ . The normals associated with these planes appear more like the bisectors of the main directions of the deviator  $\epsilon_D(t_i) - \epsilon_D(t_j)$ . The determination of the critical planes as well as the amplitude of maximized strain on these planes therefore amounts to determining the pairs of points furthest away in the sense of the Tresca norm from the loading path associated with the deviator tensor of the stresses or strains. The critical planes are then the planes whose normals are the bisectors of the difference deviator tensor associated with these pairs of points. In this present work, we chose to use the Fatemi-Socie criterion because it often appears to be very efficient in its fatigue predictions for metals [4]. The fatigue parameter of this critical plane type criterion combines the amplitude of shear strain in the planes with the maximum normal stress to these planes. The relationship with a lifespan is of the following form:

$$\frac{\Delta\gamma_{\max}}{2} \left( 1 + k \frac{\sigma_{n, \max}}{\sigma_y} \right) = \frac{\tau_f}{G} (2N)^{b_\gamma} + \gamma_f (2N)^{c_\gamma} \quad (3)$$

where  $\Delta\gamma_{\max}$  is the maximum amplitude of shear strain,  $\sigma_{n,\max}$  is the maximum tensile stress at the critical plane,  $\sigma_y$  is the elastic limit,  $G$  is the shear modulus,  $\tau_f$  is the shear fatigue resistance coefficient,  $b_\gamma$  is the shear fatigue strength exponent,  $\gamma_f$  is the shear fatigue ductility coefficient and  $c_\gamma$  is the shear fatigue ductility exponent and  $k$  is a parameter that weighs the normal stress effect on the critical plane.

The objective here is to obtain a map of the parameter around the porosities to detect the most damaging zones and predict the initiation of a crack. All calculations for this work were carried out using chronocad<sup>2</sup> ®software.

### 3 Description of loading

In order to understand the consequences of the most harmful porosities on the performance of materials, in particular sinkholes, the experimental choices were to pilot the tests with imposed plastic strain amplitude: 0.1% and 0.4%. These types of porosities, often resulting from inadequate solidification processes in metal alloys, can significantly weaken the mechanical strength of materials by creating areas of stress concentration. By imposing a plastic strain amplitude, we simulate the extreme conditions to which the material could be exposed in service, thus making it possible to directly observe the interaction between the strains and the present porosities. The process begins with a hardening phase of the material, corresponding to an increase in the elastic range. After this initial phase, the curve representing the stresses as a function of the strains stabilizes. At this stage, we exploit the stabilized curve to calibrate a Prager type constitutive law. This law is particularly suitable for modeling the behavior of materials, which undergo cyclic plastic strains, because it makes it possible to integrate kinematic hardening. In Figure 2, we specify the different phases of such a behavioral law.

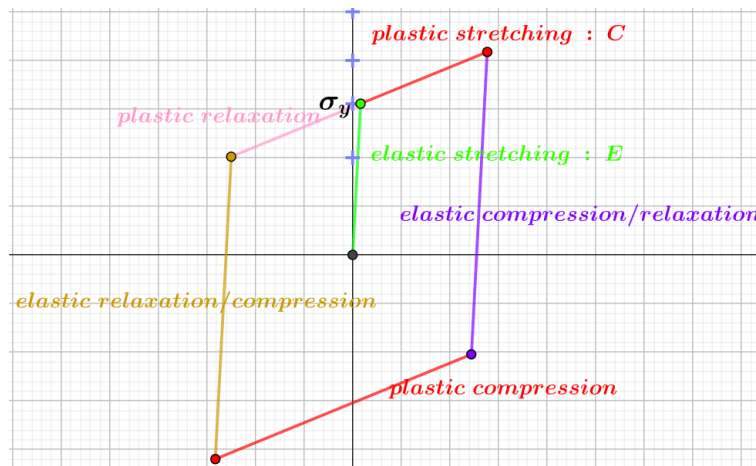


Figure 2: Prager's constitutive law

## 4 Numerical chaining up to estimation of a lifespan

We have at our disposal four tubular specimens each presenting a killer porosity: The specimens were subjected to cyclic traction/compression with a loading ratio  $R=-1$  along their axis (Oz) in order to have an imposed plastic strain amplitude of 0.1% for the first two, an imposed plastic strain amplitude of 0.4% for the last two. In this first work initiating a fatigue analysis method, we made the simplistic choice of isolating each killer porosity in a representative elementary volume (VER).

### 4.1 Setting the law of behavior with imposed plastic strain amplitude

We chose a simple Prager type model. Experimental measures show a Young's Modulus  $E = 208000$  MPa. The plastic behavior of the specimens during a semi-life cycle is represented in figure 3. The hardening coefficient  $C$  can be deduced, as well as the elastic limit  $\sigma_y$ . The results are resumed in table 1

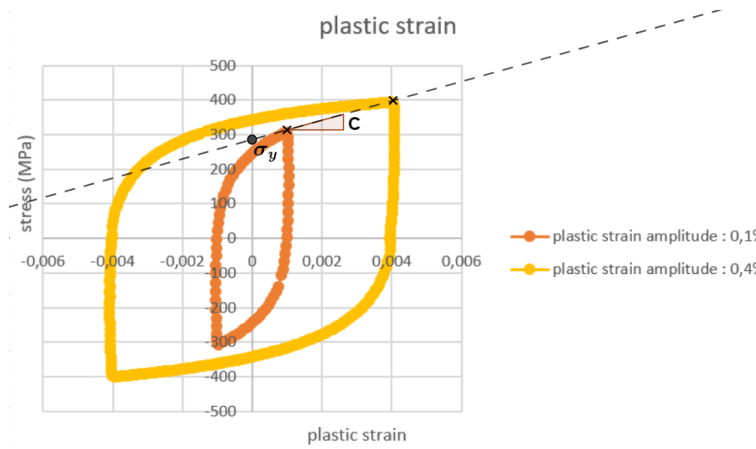


Figure 3: Plastic behavior

Table 1: Parameters of the Prager-type constitutive law

Young's modulus E	Elastic limit $\sigma_y$	Hardening parameter C
208000	296	26800

### 4.2 Creation of a VER around the porosity and cyclic loading

In a first stage of this work, we are not interested in the interaction of the porosities with each other. We therefore choose to isolate each porosity, the geometry of which is obtained by tomography, in a representative cubic elementary volume (VER) of side 10 times the largest

dimension characterizing the porosity. A refined gradual mesh around the porosity chosen with tetrahedral-quadratic elements. For each specimen, the loading is controlled in imposed displacement in order to ensure the plastic strain imposed in the experimental tests. We have summarized in table 2 the number of the test piece where the killer porosity is located, as well as the dimensions of the smallest parallelepiped encompassing the porosity, the length of the side of the VER, the number of meshes and the number of nodes of the mesh.

**Table 2:** Characteristic of the porosity and mesh of the VER

N° of specimen	L ( $\mu m$ ) along ( $Ox$ )	l( $\mu m$ ) along ( $Oy$ )	h( $\mu m$ ) along ( $Oz$ )	c	Number of meshes	Number of nodes
6-2	214	63	141	2000	98896	133643
6-5	90	100	60	1000	44494	60954
6-10	32	31	38	300	21563	30063
6-18	99	55	38	1000	37089	50958

### 4.3 Mapping of the chosen fatigue parameter

For each VER, we are interested in the zone where the fatigue parameter is the highest. The mechanisms that induce fatigue damage are not concentrated in a single point but rather in a finite volume around the point. It is therefore important to take into account the stress/strain gradient effects [6]. To this end, we will associate with each element not the value of the calculated fatigue parameter but rather the average value over all the meshes at a critical distance that we have chosen to be  $3\mu m$ . In Figures 4, 5, 6 et 7 the maps of the averaged parameter are drawn for each of the four porosities.

Table 3 summarizes the processing times for calculating the Fatemi-Socie parameter for all the elements of the mesh. The number of instants in a cycle is 20.

**Table 3:** Calculation time of the fatigue parameter on the entire mesh

N° of specimen	Number of elements	Time in seconds
6-2	98896	14.8
6-5	44494	6.7
6-10	21563	3.4
6-18	37089	5.4

### 4.4 Proposal for a lifespan law

Experimentally, the specimens were subjected to cyclic loading with imposed plastic strain amplitude until the initiation of a crack. In the table 4, we summarize for each specimen, the

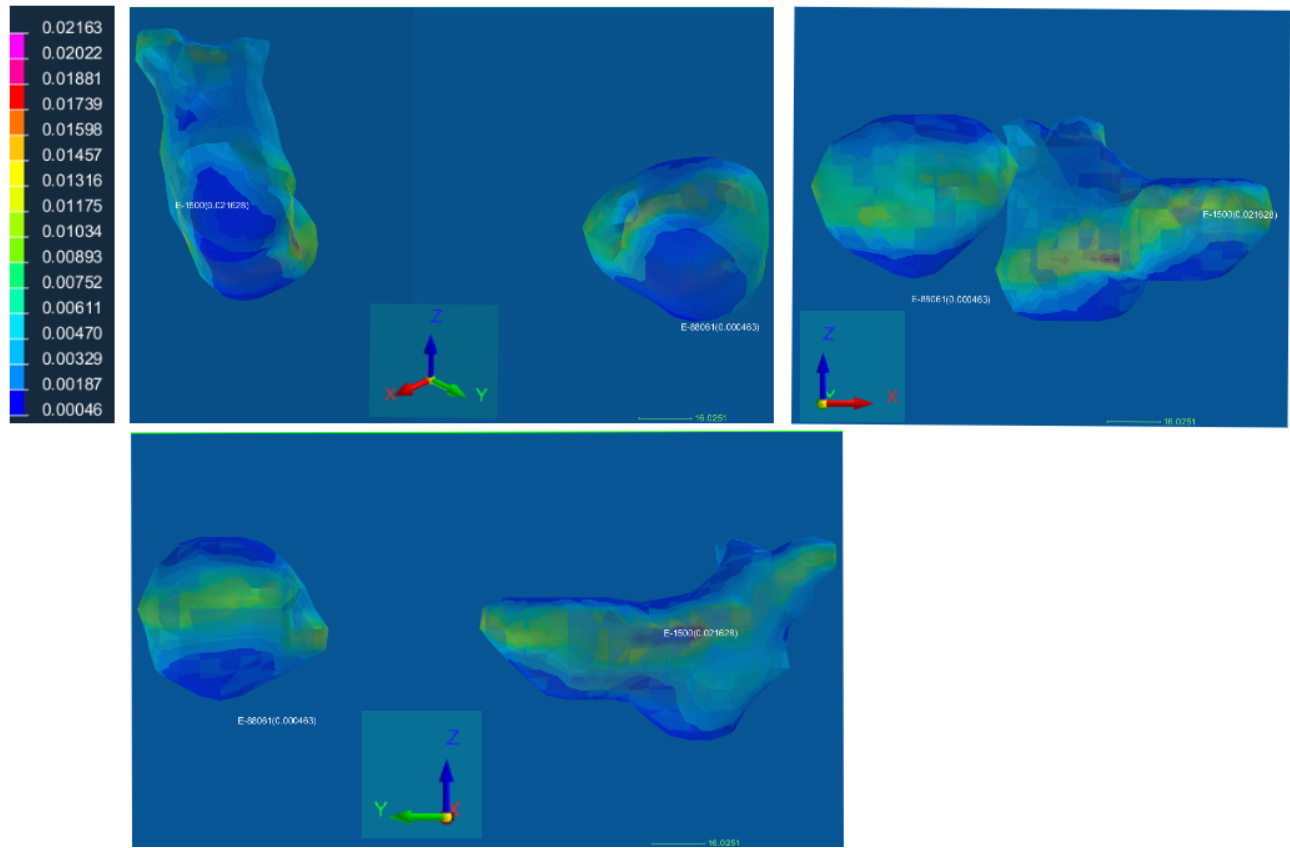


**Figure 4:** Mapping of the Fatemi-Socie parameter around the double killer porosity of specimen 6-2

level of plastic strain amplitude imposed during its cyclic loading, the maximum value of the Fatemi-Socie parameter around the killing porosity, and its experimental lifespan.

**Table 4:** Lifespan law

N° of specimen	Level of imposed plastic strain amplitude	Maximum value of the Fatemi-Socie parameter around the killer porosity	Experimental lifespan (in number of cycles)
6-2	0.1%	0.021	16719
6-5	0.1%	0.013	23496
6-10	0.4%	0.029	1571
6-18	0.4%	0.057	1741

We find graphically a power law linking the maximum value of the fatigue parameter and the lifespan (see figure 8).



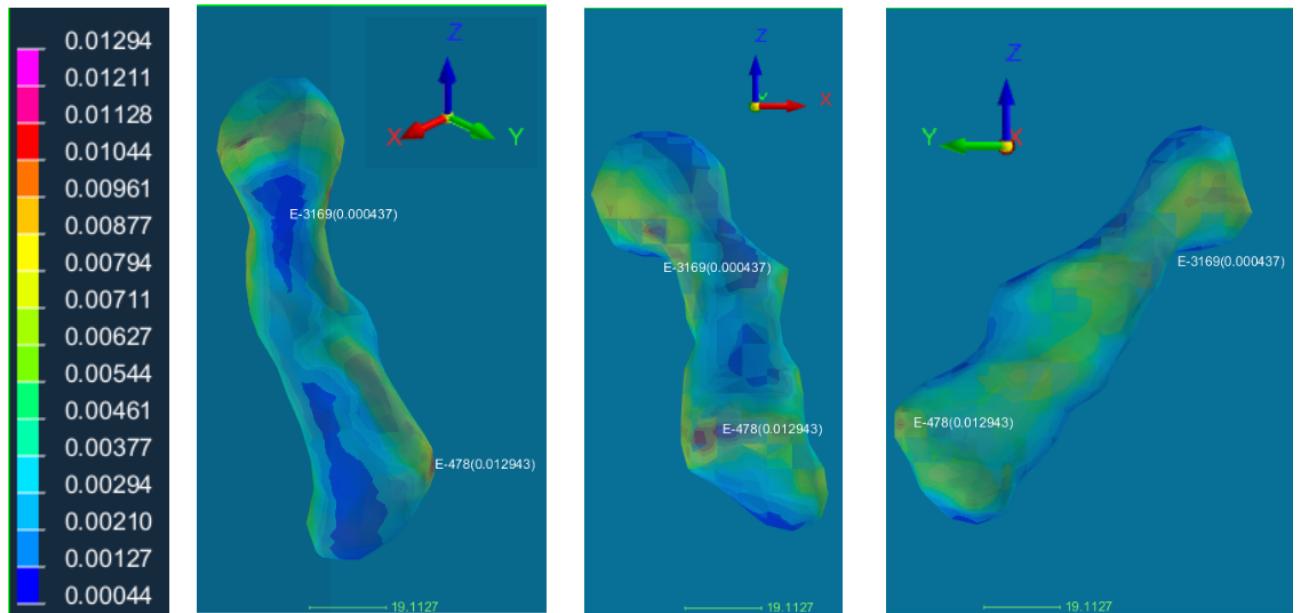


**Figure 5:** Mapping of the Fatemi-Socie parameter around the double killer porosity of specimen 6-5

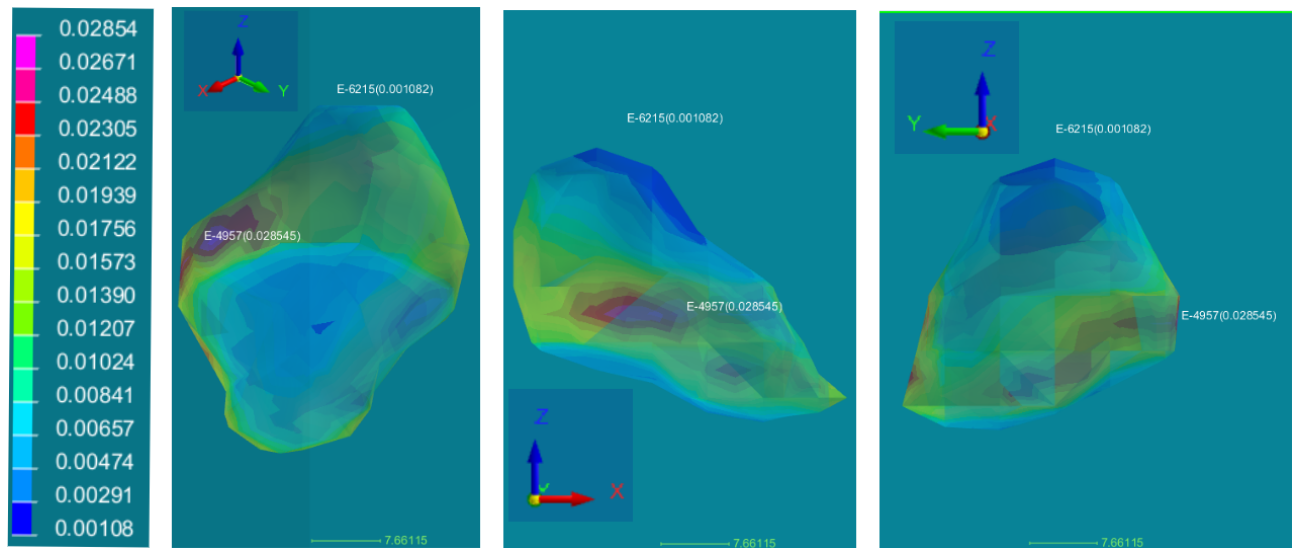


**Figure 6:** Mapping of the Fatemi-Socie parameter around the double killer porosity of specimen 6-10

## 5 Conclusion

Parts obtained from G20Mn5 cast steel have internal porosities, which significantly alter their fatigue life. In this work, we have shown the feasibility of a numerical fatigue analysis of such a part starting from the geometry of the porosity obtained by tomography up to the application of a critical plane-type fatigue criterion, through the calculation of the state of stresses and strains

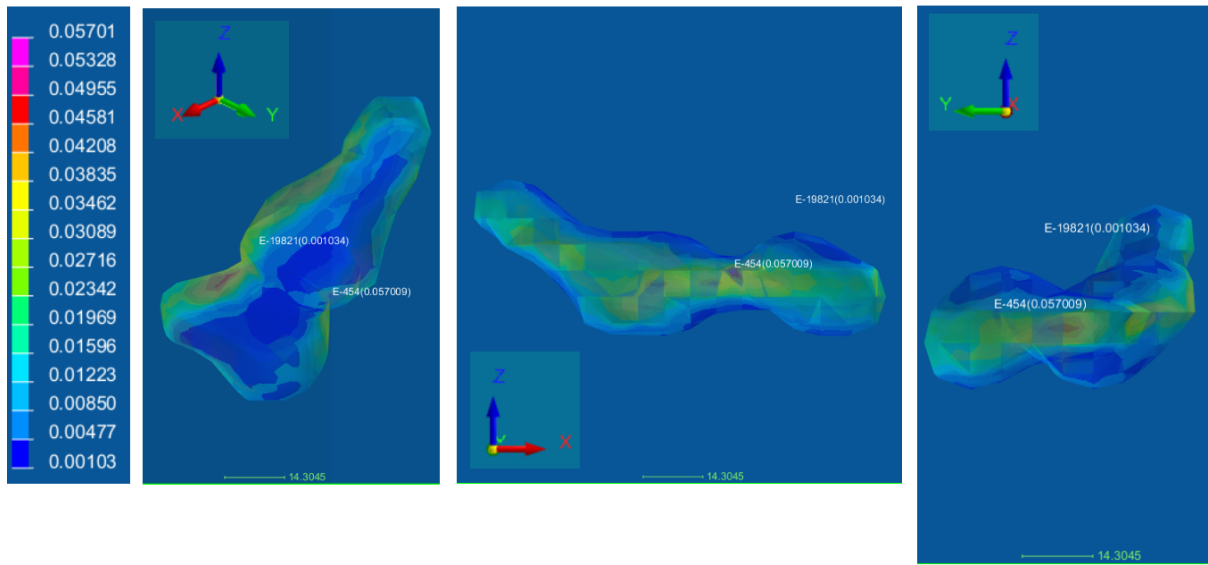


**Figure 7:** Mapping of the Fatemi-Socie parameter around the double killer porosity of specimen 6-18

during a stabilized loading cycle. The results obtained in this firstwork are promising both in terms of the necessary calculation times and the estimates of lifespans. This first study makes the simplification hypothesis of not taking into account the influence of the porosities on each other (except in the case of the specimen 6-2 where the porosity appears double), and the study did not carry only on 4 test specimens. In order to obtain a more precise and realistic lifespan law, it is crucial not to isolate the porosities but rather to study the interactions between them because they do not behave independently. The proximity of porosities can, in particular, create areas of greater stress concentration. A multiplication of the comparison of numerical and experimental tests, as well as by taking into account a greater number of porosities in the VER, will be the subject of further work, as well as the study of sensibility of the fatigue parameter to the constitutive law.

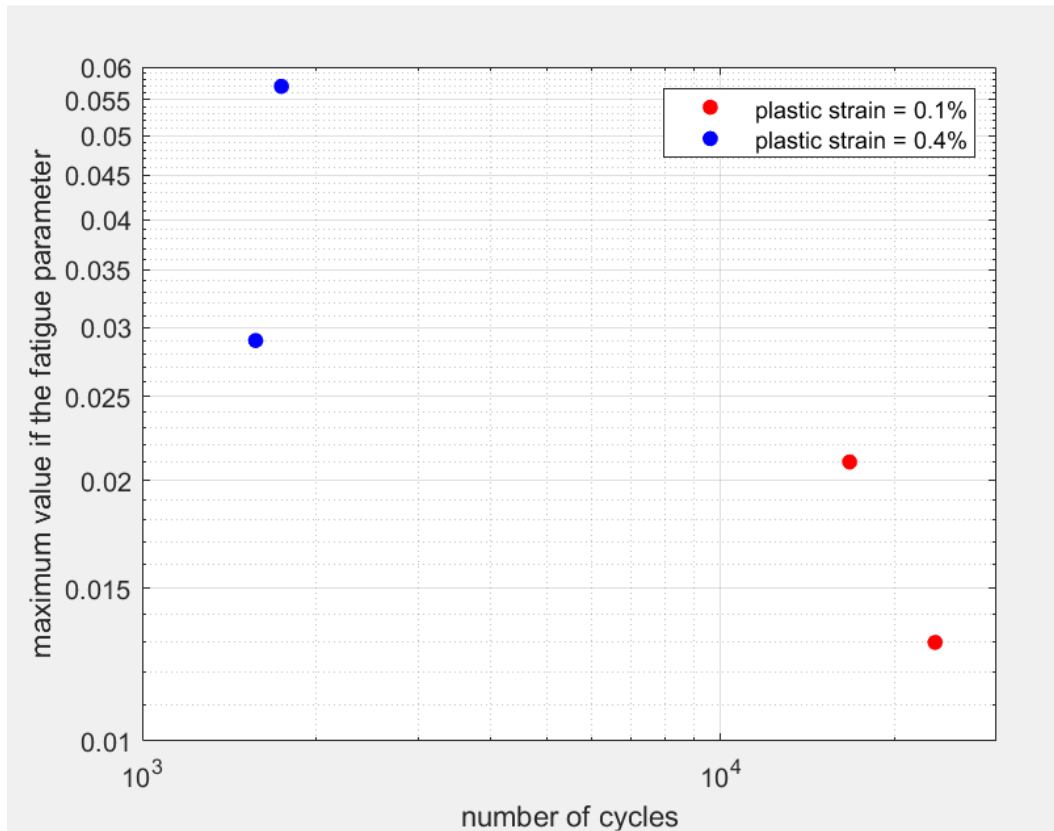


**Figure 8:** Lifespan law

## REFERENCES

- [1] Bermond, A. *Microstructure et mécanismes d'endommagement en fatigue oligocyclique de l'acier moulé G20Mn5*. Thèse de doctorat, Université de Lyon, (2022).
- [2] Bermond, A. and Roume, C. and Stolarz, J. and Lenci, M. and Carton, J.F. *Low Cycle Fatigue of G20Mn5 Cast Steel Relation between Microstructure and Fatigue Life*. Materials, (2022), vol. 15 (20), pp.7072.
- [3] Agard, B. and Giraud, L. and Fauvin, F. and Roux, J.C. and Monnet, P. and Feulvarch, E. *Fast computation of critical planes for fatigue life analysis of metals*. Compte Rendus de Mécanique, (2022), Vol. 350, p. 495-5063.
- [4] Sharifimehr, S. and Fatemi, A. *Evaluation of methods for estimating shear fatigue properties of steels and titanium alloys*. International Journal of Fatigue, (2019), Vol. 122, p. 19-34.

- [5] Cruces, A.S. and Garcia-Gonzales, A. and Moreno, B. and Itoh, T. and Lopez-Crespo, P. *Critical plane based method for multiaxial fatigue analysis of 316 stainless steel*. Theoretical and Applied Fracture Mechanics, (2022), Vol. 118, 103273.
- [6] Guerin, B. and Pessard, E. and Morel, F. and Verdu, C. *A non local approach to model the combined effects of forging defects and shot-penning on the fatigue strength of a pearlitic steel*. Theoretical and Applied Fracture Mechanics, 2018), Vol. 93, p. 19-32.